Validating Nonlinear Transducer Motor Simulations with Measurement

Jonathan Gerbet (KLIPPEL GmbH, Dresden, Germany),
Ling Chen Zhu (Pana Sound (Guang Dong) Co.),
Wolfgang Klippel (University of Technology, Dresden, Germany)

Abstract: Finite Element Analysis (FEA) is a powerful tool for predicting the behavior of electrodynamic transducers without the need for numerous physical prototypes, significantly reducing both cost and development time. However, validating FEA results remains challenging and time-consuming. In this paper, a fast, full dynamic, and non-destructive measurement technique developed by KLIPPEL is applied to validate a COMSOL-based FEA of the key parameters of the nonlinear transducer motor: the position-dependent force factor ($Bl(x)$) and the frequency- and the position-dependent lossy self-inductance ($Z_{\mathrm{L}}(f,x)$). The study compares the nonlinear motor parameters obtained from both measurement and simulation. It further identifies which of these parameters are most critical for accurately predicting transducer behavior, particularly with respect to nonlinear distortion generation and voice coil stability.

1. Introduction

Electrodynamic transducers are among the few systems in which electromagnetic behavior must be accurately understood across a very wide frequency range, from DC up to several kilohertz. They also exhibit strong nonlinearities, particularly due to the large displacement of the voice coil within the magnetic field during audio signal reproduction. Accurate modeling of this behavior is critical for loudspeaker design.

Finite Element Analysis (FEA), combined with lumped-parameter modeling, is widely used to simulate the linear and nonlinear behavior of electrodynamic transducers. Such simulations enable extensive geometry and material studies and reduce the need for physical prototyping. Their accuracy, however, is influenced by idealized assumptions, modeling simplifications, and uncertainties in material parameters. Consequently, validation against measurements of physical transducers is crucial to ensure reliable performance predictions.

Previous work has already addressed comparisons between FEA and measurements. For example, Dodd et al. [1] and Cobianchi et al. [2] used semi-static measurements to estimate the nonlinear, frequency-dependent inductance. Cobianchi also combined static and dynamic techniques to characterize $Bl(x)$. Malbos et al. [3] compared FEA with full dynamic measurements using the Klippel LSI system.

However, prior comparisons with the Klippel LSI measurement system [4] were limited because its simplified inductance nonlinearity model assumed frequency independence, an assumption that becomes invalid under broadband excitation and when shorting material is used. To address this limitation, an improved full dynamic measurement technique, Klippel Fast Large Signal Identification (FLSI) [5] was introduced in previous work [6] and is briefly described in Section 2. This method enables extraction of nonlinear, frequency-dependent parameters from physical transducers excited by broadband signals, allowing for more accurate model validation.

In Section 4, the measured parameters are used in a nonlinear lumped-parameter model driven by sinusoidal signals. The resulting nonlinear distortions (voice coil DC displacement and harmonic distortion) are compared with physical measurements and the underlying physical causes of the distortion are identified. Subsequently, the nonlinear lumped parameters are computed using the FEA software suite COMSOL Multiphysics [7] and directly compared with the measured ones, completing a full validation loop.

In this study, the FLSI measurement method is applied to an 8-inch woofer whose motor contains no shorting rings. The focus is on the nonlinear motor parameters: force factor and self-inductance.

2. Measurement

2.1. Transducer Modeling

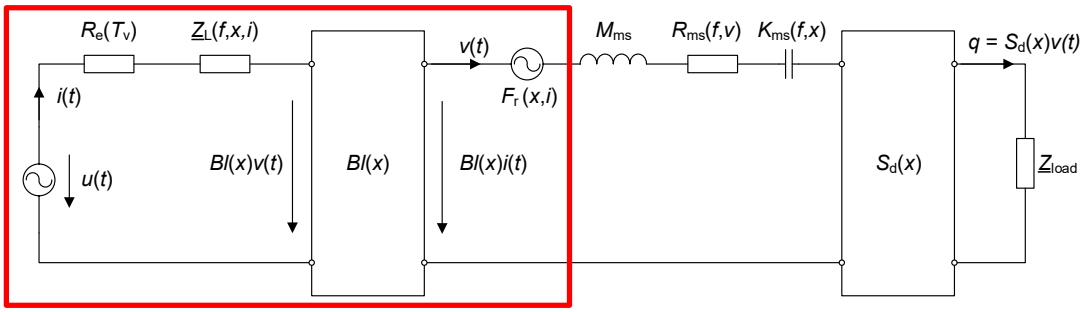

Figure 1: Nonlinear lumped-parameter model of an electro-dynamic transducer

An electrodynamic transducer can be described by a nonlinear, dynamic lumped-parameter model, as shown in Figure 1. The structure of this model reflects the fundamental physical mechanisms of the transducer, and its parameters are directly related to operating principle, design, material properties, and assembly. This approach is widely used in industry and has proven effective for predicting voice coil motion and nonlinear distortion. The present study focuses on the motor parameters, highlighted in Figure 1.

An excitation voltage $u(t)$ causes an electric current $i(t)$ to flow through the voice coil. The electromechanical force factor $Bl(x)$, which depends on voice coil displacement $x(t)$, converts this current into the *Laplace force* $Bl(x)i(t)$. This force excites a resonator consisting of the moving mass M_{ms}, a nonlinear mechanical stiffness $K_{\mathrm{ms}}(x)$, and a mechanical resistance R_{ms}, resulting in a voice coil motion of velocity $v(t)$. The diaphragm with the effective surface area $S_{\mathrm{d}}(x)$ converts this velocity into volume velocity, generating sound pressure $p(t)$. At the same time, the coil motion induces a back electromotive force (EMF) $Bl(x)v(t)$.

The coil current also generates a time-varying magnetic field, producing a self-induced voltage. Ideally, the self-inductance of the coil is constant, but in practice it varies strongly with frequency f, displacement x, and effective permeability of the iron μ_{eff}. Accurately modeling these effects over a wide bandwidth requires a complex nonlinear dynamic model whose results are difficult to interpret.

A useful simplification is to represent this complex lossy inductance as a set of *blocked impedances* at different clamped voice coil positions x_k ($k \in \mathbb{Z}$):

$$\underline{Z_{\mathrm{L}}}(f, x_k) = j\omega L(f, x_k) + R_{\mathrm{L}}(f, x_k)$$

Here, $\underline{Z_{\mathrm{L}}}(f, x_k)$ is the complex blocked impedance, comprising the pure, frequency- and displacement-dependent real-valued inductance $L(f, x_k)$ and the pure, real-valued resistance $R_{\mathrm{L}}(f, x_k)$; $j\omega$ is the complex frequency. The AC displacement component x_{AC} in the total voice coil displacement $x = x_k + x_{\mathrm{AC}}$ is ignored in this simplified representation. For clarity, also the magnetic flux modulation caused by nonlinear permeability is omitted here.

This blocked-impedance model is advantageous because it provides interpretable parameters and can be identified not only by full dynamic measurements but also by semi-static point-by-point measurements and simulations [6], as described in Section 3.

Two primary nonlinear effects arise from the nonlinear lossy inductance:

1. **Intermodulation Distortion**: Intermodulation distortion arises from the displacement-dependent variation of the voice coil impedance $\underline{Z_{\mathrm{L}}}(f, x)$. Of particular relevance for audibility is the variation in impedance magnitude $|\underline{Z_{\mathrm{L}}}(f, x)|$, which produces amplitude modulation at high frequencies and, to a lesser extent, harmonic distortion in the output signal. The impedance magnitude is also used to define the maximum permissible displacement, x_{L}, limited by nonlinear distortion, as specified in IEC 62458 [8].
2. **Force caused by self-inductance (*Reluctance Force*)**: Non-uniformity of the alternating (AC) magnetic field along the coil axis produces a reluctance force, which causes static (DC) displacement and harmonic distortion. Among these effects, the DC displacement is dominant for typical audio signals: although the DC and AC distortion energies are comparable, the AC distortion is distributed across harmonics, while the DC displacement is concentrated entirely at zero frequency.

The reluctance force is related to the spatial gradient of the pure inductance and can be approximated by:

$$F_{\mathrm{r}}(f, x, i) \approx \frac{1}{2}\left(\frac{\mathrm{d}L(f, x)}{\mathrm{d}x} i^2\right)$$

This expression holds under the assumption of low iron losses in the frequency range of interest, typically at low frequencies where the reluctance force is most relevant. This assumption is valid for the transducer investigated here. A more general equation applicable to a wider class of transducers is given in [6].

The nonlinear effects described above cannot be directly measured using voltage sensors, triangulation lasers, or microphones, since all nonlinear mechanisms are coupled and not independently observable. Therefore, a model-based approach, as illustrated in Figure 1, is required to decompose and isolate the individual contributions. This enables a clear identification of the sources of undesired behavior and supports targeted optimization of transducer design.

2.2. Measurement Procedure

The full dynamic measurement method used in this work was introduced in previous work [6]. It employs a multi-tone excitation signal to stimulate the transducer simultaneously at multiple frequencies across the audio range.

The transducer used in this study was an 8" woofer, mounted in a measurement stand that also accommodates a laser and a microphone. Figure 2 shows the measurement setup, including the transducer under study. The most relevant coil and gap dimensions of the transducer are summarized in Table 1:

Figure 2: Measurement setup of device under study

Table 1: Dimensions of the voice coil and gap

Voice coil height	15.1 mm
Voice coil inner diameter	30.5 mm
Gap height	5 mm
Gap width	2.35 mm

The transducer is connected to the Klippel Analyzer 3 [9]. This measurement device receives the stimulus signal from a PC, amplifies it internally, and drives the transducer. Voltage, current, displacement, and sound pressure are recorded simultaneously and transferred to the PC for processing. Dominant linear and nonlinear lumped parameters are obtained by fitting a parameterized model to the measured electrical current, minimizing

$$\epsilon(t) = i_{\mathrm{meas}}(t) - i_{\mathrm{model}}(t)$$

in a least-squares sense to yield the optimal parameter set.

3. Finite Element Analysis

The COMSOL Multiphysics software suite was employed to simulate the displacement-dependent parameters of the motor. The simulation procedure followed the methodology outlined in *Modeling Speaker Drivers in COMSOL Multiphysics* [10]. The rotational symmetry of the transducer under investigation was utilized to reduce computational complexity.

The radial magnetic flux density B_r at the coil radius r is first obtained from a stationary magnetic simulation. The force factor $Bl(x_k)$ at given voice coil positions x_k is then computed by averaging the product of B_r and the total wire length l over the voice coil height h:

$$Bl(x_k) = \frac{1}{h}\int_{x_k-h/2}^{x_k+h/2} B_r(z, x_k) \cdot l \, \mathrm{d}z,$$

where z is the axial coordinate pointing in the direction of voice coil movement. The total wire length of the coil is

$$l = 2\pi r N_0,$$

with N_0 denoting the number of turns. The voice coil position x_k was varied from -7 mm to +7 mm in discrete steps.

To compute the self-inductance, a blocked-coil approach is used, in which the coil velocity is constrained to zero, eliminating motional EMF. As in the computation of the nonlinear force factor, the coil is shifted to different positions. At each position, the voice coil is excited with a harmonic AC voltage. Then, the perturbated magnetic field (including the static component from the permanent magnet and the alternating component of the voice coil current), and the currents induced in the electromagnetic circuit are solved. The simulation returns the complex blocked-coil impedance $\underline{Z_\mathrm{L}}(f, x_k)$ at each fixed coil position x_k.

4. Results

4.1. Lumped-Parameter Measurement and Simulation

Before comparing FEA with measurements, it is essential to verify that both the measurement data and the underlying lumped-parameter model accurately represent the transducer's physical behavior. First, error metrics are defined to quantify the agreement between measured and modeled states obtained during parameter identification. Second, independent excitation signals (distinct from the multi-tone used for identification) are applied to the lumped-parameter model in Figure 1, and the resulting nonlinear distortion mechanisms are compared with measurements.

4.1.1. Validation of Measurement and Model

The nonlinear parameter measurement described in Section 2.2 uses a multi-tone stimulus and optimizes the error between measured and modeled current $i(t)$ to fit optimal parameters. The deviation between these signals provides an estimate of the accuracy of both the lumped-parameter model and the identification of its free parameters. A commonly used single-value metric to evaluate this deviation is the normalized root mean square error (NRMSE). For the electrical current, it is defined as

$$NRMSE(i) = \frac{\int_0^T (i_\mathrm{meas}(t) - i_\mathrm{model}(t))^2 \, \mathrm{d}t}{\int_0^T i_\mathrm{meas}(t)^2 \, \mathrm{d}t} \times 100\%$$

where T denotes the duration of the multi-tone excitation signal. In addition, a laser triangulation sensor was used to measure the physical voice coil displacement $x(t)$. This is

particularly important because most nonlinear parameters are displacement-dependent. Accurate identification therefore requires a low displacement modeling error. The corresponding NRMSE for displacement is given by:

$$NRMSE(x) = \frac{\int_0^T (x_{\mathrm{meas}}(t) - x_{\mathrm{model}}(t))^2 \,\mathrm{d}t}{\int_0^T x_{\mathrm{meas}}(t)^2 \,\mathrm{d}t} \times 100\%$$

As shown in Table 2, the identification errors for both current and displacement were below 2 %. This indicates very good agreement between model and measurement.

Table 2: Parameter Identification Errors

Parameter	**NRMSE**
$NRMSE(i)$	1.70 %
$NRMSE(x)$	0.81 %

4.1.2. Single Tone Measurements and Simulations

To verify that the identified nonlinear lumped parameters (Figure 1) are independent of the excitation signal and measurement conditions, the model was validated using single-tone stimuli that differ substantially from the multi-tone signal used for parameter identification. Moreover, these lumped-parameter simulations enable systematic parameter studies that help to reveal the physical origins of unwanted distortion.

For these simulations, the Klippel SIM software [11] was used. This tool applies the identified linear and nonlinear parameters to simulate state variables such as current, displacement, and sound pressure. The simulations were performed using the measured parameters shown in Figures 8 and 10.

The transducer was driven with a stepped-sine stimulus, in which multiple frequencies are excited sequentially, but only one frequency is excited at a time. The RMS voltage was set to achieve a peak voice coil displacement of 7 mm – below the mechanical limit, yet sufficient to induce significant nonlinear distortion.

For DC displacement investigations, the RMS voltage of the stimulus was set to 16 V. Since this level would exceed the maximum displacement range of the transducer, the measurement bandwidth was restricted to 50-400 Hz, while the lowest simulation frequency was set to 20 Hz.

The results are shown in Figure 3, which shows the maximum positive (*peak*) and minimum negative (*bottom*) displacement versus frequency. Figure 4 shows the corresponding instantaneous DC displacements caused by nonlinear behavior, calculated from one period T of the displacement waveform $x(t)$ at each frequency f:

$$x_{\mathrm{DC}}(f) = \frac{1}{T}\int_0^T x(t,f) \,\mathrm{d}t$$

In addition to the full simulation, Figure 4 also presents simulations with individual parameters activated while others are disabled, in order to identify the root cause of the observed DC components. The corresponding results are discussed in the next section.

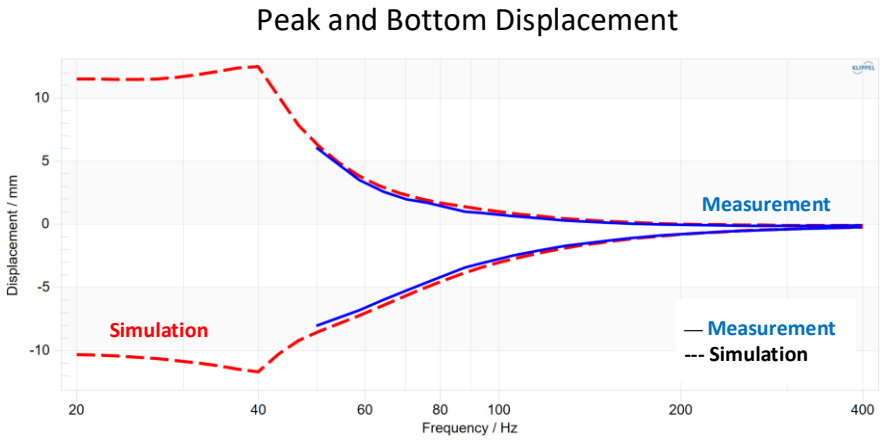

Figure 3: Simulated and measured peak and bottom displacement

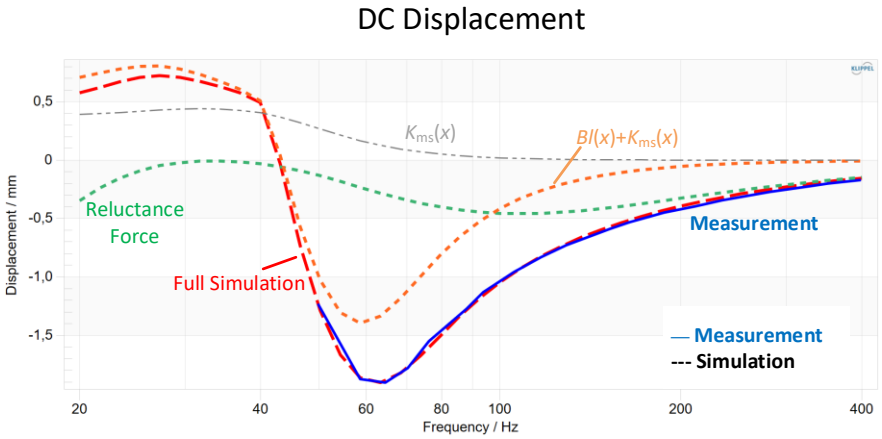

Figure 4: DC displacement x_{DC} over frequency f

The SIM tool also calculates harmonic distortion in the sound pressure simultaneously to the displacement simulation. Measurements were carried out using a ¼" microphone positioned 20 cm in front of the transducer to ensure a high signal-to-noise ratio. For both measurement and simulation, the stimulus voltage was reduced to 8 V in order to extend the usable measurement bandwidth towards lower frequencies.

Figure 5 and Figure 6 show the relative second- and third-order harmonic distortion for both measurement and simulation. Across most of the investigated frequency range (20 Hz < f < 200 Hz), deviations remain below two percentage points and never exceed four percentage points, demonstrating excellent agreement.

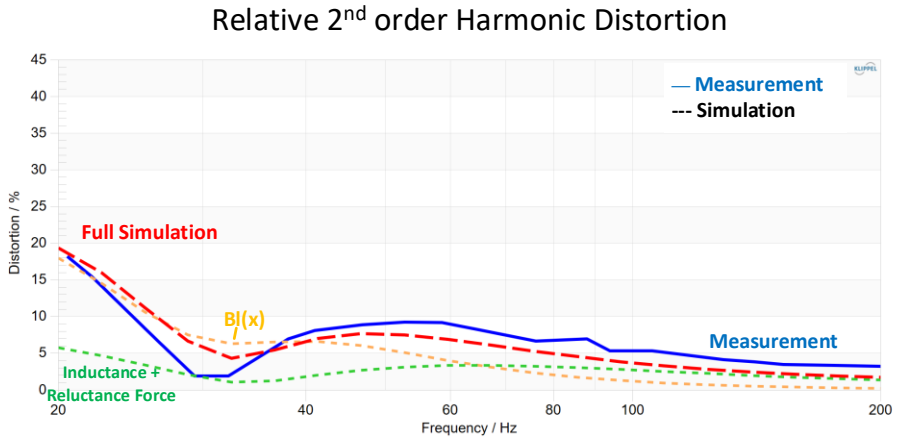

Figure 5: Measured and simulated 2nd order harmonic distortion in the sound pressure

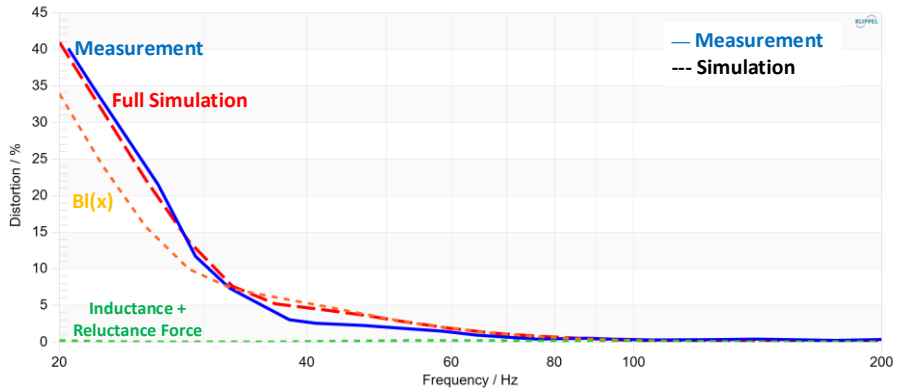

Figure 6: Measured and simulated 3rd order harmonic distortion in the sound pressure

4.1.3. Discussion

DC displacements are unwanted nonlinear distortion components that are critical for loudspeaker performance, as they can limit peak displacement and reduce robustness. The DC displacement simulation closely matches the measurements.
In addition, identifying the causes of DC displacements aids in developing remedies to improve transducer performance. Figure 4 shows simulations in which selected nonlinear parameters were activated or deactivated. The results can be interpreted as follows:

- **Below resonance ($f < f_s \approx 40$ Hz):** The asymmetric $Bl(x)$ generates a DC force, pushing the voice coil out of the gap toward the maximum of the $Bl(x)$ curve.
- **At resonance:** $Bl(x)$ cannot produce a DC force because displacement and current are orthogonal. A slightly asymmetric $K_{\mathrm{ms}}(x)$ contributes a DC component at low frequencies where displacement is high.
- **Slightly above resonance:** A negative DC force produced by $Bl(x)$ pushes the voice coil toward the back plate, away from its maximum value.
- **Above ~100 Hz:** The reluctance force dominates, moving the voice coil toward the maximum of the nonlinear inductance $L(f, x)$.

Harmonic distortion simulations also match the measurements closely, confirming that the lumped-parameter model and identified parameters describe the transducer with good accuracy. As with DC displacement, the causes of harmonic distortion can be deduced from simulations (Figures 5 and 6):

- **Second-order distortion:** Caused primarily by asymmetric nonlinearities, mainly the asymmetric shapes of $Bl(x)$ and $\underline{Z_{\mathrm{L}}}(f,x)$. Harmonic distortion from reluctance force is minor, only slightly exceeding 1 % (not explicitly shown in the chart).
- **Third-order distortion:** Predominantly caused by symmetric nonlinearities, with $Bl(x)$ being the dominant contributor. Inductance and reluctance force have negligible impact on third-order harmonic distortion, as the symmetric part of the inductance is small.
- **Frequency dependency:** $Bl(x)$ distortion is significant only at low frequencies where displacement is large, while reluctance force contributes harmonic distortion above resonance because it depends on $i(t)^2$, which is relevant also at higher frequencies.

4.2. Comparison between FEA and Measurement

Figure 7 shows the motor assembly and the simulated magnetic field generated by the permanent magnet in COMSOL. Based on this simulation, the force factor $Bl(x)$ is calculated according to the procedure described in Section 3.

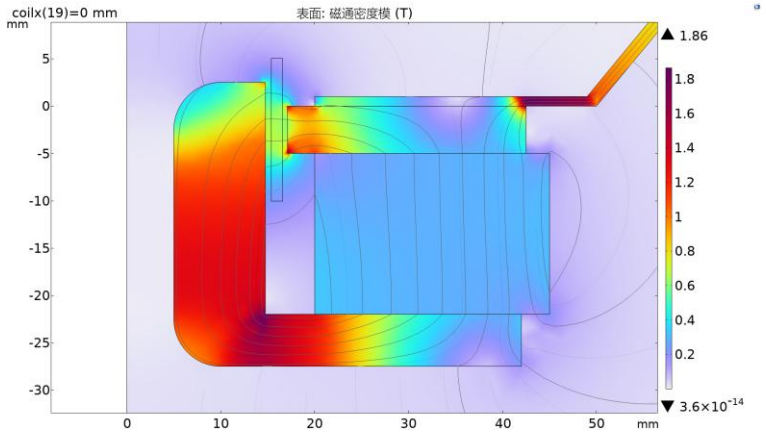

Figure 7: Flux density generated by the permanent magnet in the transducer under investigation

Figure 8 compares force factor curves obtained from measurement and FEA. Since the manually assembled transducer's voice coil was not positioned at the optimal rest position, the measured curve was virtually shifted outward the gap by 1.7 mm to the corrected position x_0' (curve had to be shifted in negative direction) before comparison. The maximum relative deviation

$$\Delta_{\max}^{\mathrm{rel}}(Bl(x_k)) = \max_k \left(\frac{|Bl_{\mathrm{meas}}(x_k) - Bl_{\mathrm{FEA}}(x_k)|}{|Bl_{\mathrm{meas}}(x_k)|} \right)$$

is smaller than 4 %.

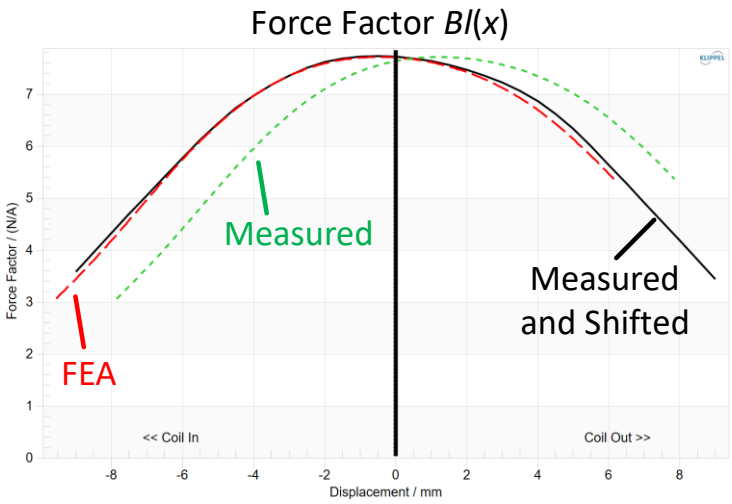

Figure 8: $Bl(x)$ curves obtained by FEA and measurement

Figure 9 shows the magnitude and phase of the impedance of the lossy inductance over frequency at the voice coil rest position. As in the force factor investigation, the measured impedance is evaluated at the corrected position x_0'. Deviations between simulation and measurement are small: the maximum magnitude error is below 4 %, and the phase varies by no more than 5 degrees across the investigated bandwidth (f < 1 kHz).

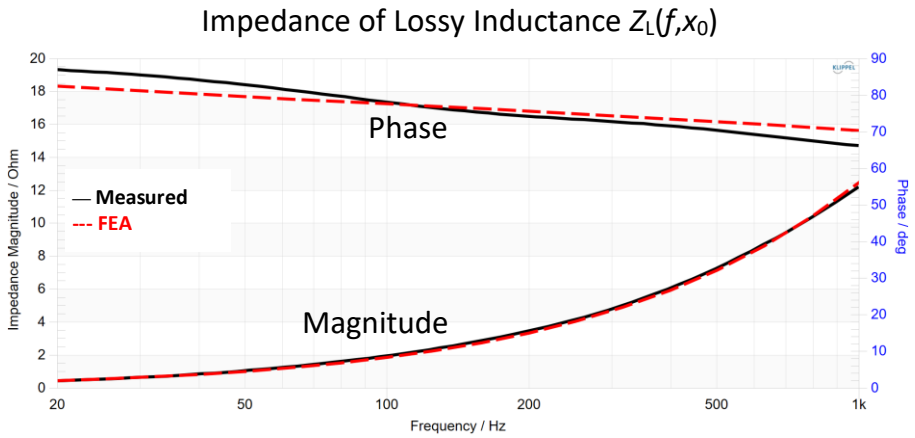

Figure 9: Magnitude and phase of the impedance of the lossy inductance over frequency at the voice coil rest position

Figure 10 shows the displacement-dependent impedance magnitude curves of the nonlinear lossy self-inductance at various frequencies. To enable direct comparison, the measured nonlinear curves were shifted in the same manner as for the force factor analysis, aligning the simulated and measured voice coil rest positions. At rest position, measurement and simulation exhibit excellent agreement (see Table 3), particularly at lower frequencies. For positive displacements (coil moving out of the gap, away from the backplate), the agreement remains good. For negative displacements (coil moving toward the backplate), however, deviations increase and exceed 10 % at higher frequencies.

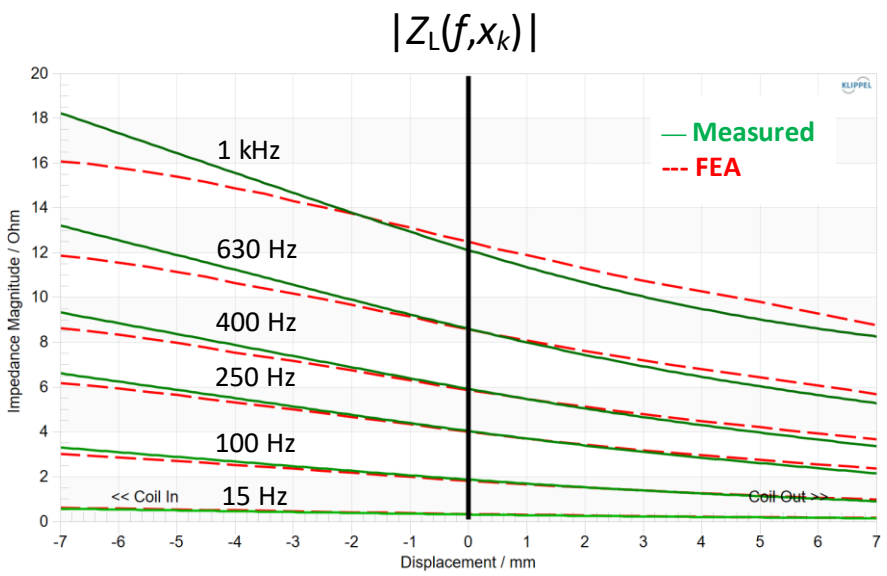

Figure 10: Modeled (FEA) and measured nonlinear impedance magnitude of the lossy inductance at various frequencies

Table 3: Deviation between FEA and Measurement

Error Metric	**Error**
Maximum relative error $\Delta^{\mathrm{rel}}_{\max}(Bl(x_k))$	< 4 %
Maximum phase error $\Delta^{\phi}_{\max}(\angle Z(f,x_k))$ at $x_k = 0$ mm	< 5°
Maximum relative error $\Delta^{\mathrm{rel}}_{\max}(\lvert Z(f,x_k)\rvert)$ at $x_k = -7$ mm	< 15 %
Maximum relative error $\Delta^{\mathrm{rel}}_{\max}(\lvert Z(f,x_k)\rvert)$ at $x_k = 0$ mm	< 4 %
Maximum relative error $\Delta^{\mathrm{rel}}_{\max}(\lvert Z(f,x_k)\rvert)$ at $x_k = 7$ mm	< 9 %

4.3. Discussion

$Bl(x)$ predicted by the semi-static FEA procedure shows excellent agreement with the full dynamic measurement. This indicates that motor geometry, coil properties, magnetization strength, permeability of the iron, and other parameters closely match the real materials, and that the FEA configuration is accurate.

The self-inductance also agrees well when the voice coil is moved out of the gap. Deviations increase, however, when the coil moves inward toward the back plate. Possible reasons include:

- Slight mismatches between material parameters in the model and reality, affecting the accuracy of the eddy current simulation.
- Minor differences between the prototype assembly and the theoretical model, causing deviations primarily at higher frequencies.
- Different excitation signals are used in measurement and FEA: the full dynamic measurement uses a high-amplitude broadband AC signal, whereas the FEA employs low-amplitude single sinus tones.
- Deviations may arise due to simplifications and modeling errors within the parameter identification algorithm used in the measurement.

5. Conclusion

This study has demonstrated a methodology for comparing frequency-dependent nonlinear motor parameters of electrodynamic transducers obtained from measurement and FEA. First, a full dynamic measurement was performed, and the resulting lumped-parameter model was validated by:

1. Evaluating the deviation between measured and modeled signals for the same multi-tone stimulus used in parameter identification.
2. Applying single tones to the lumped-parameter model and comparing the predicted harmonic distortion and DC displacement with measurements.

These comparisons demonstrate the accuracy with which the identified parameters capture the real physical behavior. For the device studied, the identified lumped-parameter model closely matched measurements at low frequencies, where the diaphragm moves like a piston.
Second, the procedure for obtaining nonlinear lumped parameters from FEA was outlined, along with the method for comparing them to measurements. Overall, FEA agreed well with measurements. Notable deviations occurred only in the self-inductance when the coil was positioned deeply within the magnetic gap. Potential causes – such as systematic discrepancies between the parameter extraction methodologies (full dynamic measurement versus point-by-point FEA) and discrepancies in material parameters – were discussed in section 4.3. These findings highlight that FEA is a powerful tool for reducing development time and cost. However, validation against measurements remains essential.

At present, transient finite element simulation is not practical for fully computing nonlinear dynamic effects, such as DC displacement for arbitrary stimuli, because time-domain simulations can require many hours depending on model complexity and signal characteristics, making large-scale parameter studies costly. For such applications, using a lumped-parameter model with parameters obtained from either FEA or measurements is more practical. As described in Section 4.2, this approach enables rapid parameter studies, including isolation of individual nonlinearities (e.g., force factor, self-inductance, or reluctance force) while disabling others. Such isolation helps to identify the specific contribution of each nonlinearity and supports targeted design improvements by focusing on the most influential parameters.

6. References

[1] Dodd, Mark; Klippel, Wolfgang; Oclee-Brown, Jack; Voice Coil Impedance as a Function of Frequency and Displacement [PDF]; KEF Audio UK (Ltd), Maidstone, Kent, UK ; Klippel GmbH, Dresden, Germany; Paper 6178; 2004 Available: https://aes2.org/publications/elibrary-page/?id=12835

[2] Cobianchi: Modelling the Electrical Parameters Of A Loudspeaker Motor System With The AC-DC Module

[3] Malbos: Prediction of the Loudspeaker Total Harmonics Distortion Using Comsol Multiphysics

[4] S52 Klippel LSI3 Specification; Klippel GmbH; https://www.klippel.de/products/rd-system/modules/lsi3-large-signal-identification.html

[5] S75 Klippel FLSI Pro Specification; Klippel GmbH; https://www.klippel.de/products/rd-system/modules/fast-large-signal-identification-professional-flsi-pro.html

[6] Gerbet, Jonathan; Klippel, Wolfgang; Measuring the nonlinear, lossy, frequency-dependent voice coil inductance]; Klippel GmbH, Dresden, presented at ISEAT conference 2024

[7] https://www.comsol.de/
[8] Sound System Equipment – Electroacoustical Transducers – Measurements of Large Signal Parameters, Standard IEC 62458
[9] H3 Klippel Analyzer 3 Specification; Klippel GmbH; https://www.klippel.de/products/rd-system/analyzer-hardware/ka3-klippel-analyzer-3.html
[10] https://www.comsol.com/support/learning-center/article/Calculating-the-Small-Signal-Parameters-of-a-Speaker-Driver-from-Finite-Element-Analysis-88011/202
[11] S3 Klippel SIM Specification; Klippel GmbH; https://www.klippel.de/products/rd-system/modules/sim-simulation.html

The Authors

Jonathan Gerbet was born in Germany in 1988. He studied electrical engineering at the Dresden University of Technology. After his studies, he joined the Klippel GmbH in 2015 as research and development engineer in the field of nonlinear active control of loudspeakers. His main field of work is loudspeaker modeling, simulation, and measurement and linear and nonlinear system identification.

Ling Chen Zhu received dual Bachelor's degrees in Automotive Design and Computer Science from Beijing University of Technology. He has held engineering and management positions at Beijing Gospel, Vifa/Scan-Speak (Denmark), and Leadtek Electronics, and is currently General Manager of PANA SOUND. Since 2009 he has represented Loudsoft, and since 2019 COMSOL Multiphysics and Klippel in China. His expertise includes driver unit design and optimization, advanced speaker and system manufacturing processes, component and material modeling, computational numerical simulation, and DSP development.

Wolfgang Klippel studied electrical engineering at the University of Technology in Dresden, in the former East Germany, where his initial studies focused on speech recognition. Afterward, he joined a loudspeaker company in eastern Germany, where he was engaged in transducer modeling, acoustic measurement, and psychoacoustics. He returned to his studies and received a Ph.D in Technical Acoustics in 1987.

After a post-doctoral year at the Audio Research Group in Waterloo, Canada, and working at Harman/JBL in Northridge, CA, he returned to Dresden in 1997 and founded Klippel GmbH. This company develops novel control and measurement systems for loudspeakers and other transducers.

Dr. Klippel has also been engaged as Professor of Electro-acoustics at the University of Technology in Dresden since 2007. His papers and tutorials on loudspeaker modeling and measurement – particularly those on large-signal behavior and physical distortion mechanisms – are considered reference works in the field.